Two algorithms to compute projected correlation functions in molecular simulations

A. Carof, Rodolphe Vuilleumier, Benjamin Rotenberg

Two algorithms to compute projected correlation functions in molecular dynamics simulations

Antoine Carof, Rodolphe Vuilleumier, and Benjamin Rotenberg

Citation: The Journal of Chemical Physics **140**, 124103 (2014); doi: 10.1063/1.4868653
View online: http://dx.doi.org/10.1063/1.4868653
View Table of Contents: http://scitation.aip.org/content/aip/journal/jcp/140/12?ver=pdfcov
Published by the AIP Publishing

Two algorithms to compute projected correlation functions in molecular dynamics simulations

Antoine Carof,[1,2] Rodolphe Vuilleumier,[3] and Benjamin Rotenberg[1,2]
[1]*Sorbonne Universités, UPMC Univ Paris 06, UMR PHENIX, F-75005 Paris, France*
[2]*CNRS, UMR PHENIX, F-75005 Paris, France*
[3]*UMR 8640 CNRS-ENS-UPMC PASTEUR, Département de Chimie, Ecole Normale Supérieure, 24 rue Lhomond, F-75231 Paris, France and UPMC Univ Paris 06, UMR 8640 CNRS-ENS-UPMC PASTEUR, F-75005 Paris, France*

(Received 18 December 2013; accepted 5 March 2014; published online 24 March 2014)

An explicit derivation of the Mori-Zwanzig orthogonal dynamics of observables is presented and leads to two practical algorithms to compute exactly projected observables (e.g., random noise) and projected correlation function (e.g., memory kernel) from a molecular dynamics trajectory. The algorithms are then applied to study the diffusive dynamics of a tagged particle in a Lennard-Jones fluid, the properties of the associated random noise, and a decomposition of the corresponding memory kernel. © *2014 AIP Publishing LLC*. [http://dx.doi.org/10.1063/1.4868653]

I. INTRODUCTION

The influence of the environment on the dynamics of a sub-system has two components: a random force that the environment exerts on the small system and a friction force, a feedback that describes the response of the environment to the dynamics of the sub-system.[1] This response of the environment is not in general instantaneous but is retarded, the environment keeping a memory of the past dynamics of the sub-system. The contraction of information that occurs when only the dynamics of the sub-system is considered was formalized by Mori and Zwanzig, who introduced the formalism of projection operators to single out the relevant degrees of freedom.[2–5] This approach provides not only the generalized Langevin equation governing their evolution, but also an explicit expression for the memory kernel describing the retarded force: The fluctuation-theorem stipulates that it is equal to the correlation function of the random force.

Recent experimental developments in particle tracking have allowed for the measurement of the random force on colloidal particles, thereby providing the first experimental tests of theoretical models for the memory of the environment based on hydrodynamic considerations.[6] However, the determination of memory kernels and extraction of the random force from molecular simulations have remained elusive. The difficulty arises from the fact that the orthogonal dynamics entering the definition of the memory kernels cannot be described as a flow in phase space and one needs to propagate observables instead of configurations.[7,8] The usual method to extract the memory kernels is thus through inversion of the Generalized Langevin Equations (GLE) using Laplace transforms or through a rewriting of the GLE as a Volterra equation.[9–14] However these methods do not allow for a decomposition of the memory kernel into different contributions. Another approach consists in fixing the sub-system, by assigning to it an infinite mass: The memory kernel then becomes a standard correlation function and a decomposition is performed easily.[15,16] However this approach modifies the dynamics of the system.

We describe here two algorithms to extract memory kernels from molecular dynamics simulations by explicitly propagating observables according to the orthogonal dynamics. We illustrate these algorithms on a simple case, namely, the Brownian motion of a tagged particle immersed in a Lennard-Jones (LJ) fluid. By performing explicitly the projection operation introduced by Mori and Zwanzig, we are able to extract the random force, which allows for a direct test of its properties at atomic scales.

The paper is organized as follows. In Sec. II we describe the theory of Mori-Zwanzig projection operators and introduce two algorithms to compute orthogonal dynamics of observables. We then discuss some statistical properties of the Mori-Zwanzig random force. In Sec. III, we present numerical results for the diffusion of a tagged particle in a Lennard-Jones fluid. We study the corresponding friction kernel, some properties of the random force and, finally, a decomposition of the friction kernel in short- and long-range contributions.

II. THEORY

A. Mori-Zwanzig projection

The Mori-Zwanzig theory is a framework to describe the evolution of any observable given the evolution of a set of "relevant" or "macroscopic" variables.[1] Typical examples of the former include the properties of a tagged particle,[4,10,13] while the latter generally refer to collective variables such as coarse-grained density, momentum, and stress fields to derive hydrodynamic equations.[12,14] While the discussion below is very general, we will consider as a practical application the case of diffusion of a tagged particle in a fluid and use its momentum as the relevant variable. We will therefore use the notation $\mathbf{P}$ for a generic relevant (set of) variables. An observable $\mathbf{B}$ is a phase space function $\mathbf{B}(\mathbf{q}, \mathbf{p})$ of the atomic positions $\mathbf{q} = (q_1, \ldots, q_n)$ and momenta $\mathbf{p} = (p_1, \ldots, p_n)$. Here

we consider a Hamiltonian system, which evolves according to

$$\begin{cases} \dfrac{\mathrm{d}q_i^t}{\mathrm{d}t} = \dfrac{\partial \mathcal{H}}{\partial p_i}(\mathbf{q}^t, \mathbf{p}^t) \\ \dfrac{\mathrm{d}p_i^t}{\mathrm{d}t} = -\dfrac{\partial \mathcal{H}}{\partial q_i}(\mathbf{q}^t, \mathbf{p}^t) \end{cases}, \tag{1}$$

with $\mathcal{H}(\mathbf{q}, \mathbf{p})$ the Hamiltonian and where $(\mathbf{q}^t, \mathbf{p}^t)$ refer to the positions and momenta after a time t, starting from the initial phase state point $(\mathbf{q}, \mathbf{p})$. The value of the observable $\mathbf{B}$ at this later time, denoted by $\mathbf{B}_t(\mathbf{q}, \mathbf{p}) = \mathbf{B}(\mathbf{q}^t, \mathbf{p}^t)$, evolves according to the Liouville equation $\dfrac{\mathrm{d}\mathbf{B}_t}{\mathrm{d}t} = \dot{\mathbf{B}}_t = i\mathcal{L}\,\mathbf{B}_t$, where $i\mathcal{L} = \{\mathcal{H}, \cdot\}$ is the Liouvillian super-operator, with $\{\cdot, \cdot\}$ the Poisson bracket. This equation may be formally integrated to give the evolution of $\mathbf{B}$: $\mathbf{B}_t = e^{i\mathcal{L}t}\mathbf{B}_0$.

The purpose of the Mori-Zwanzig formalism is to express the evolution of $\mathbf{B}$ only in terms of that of the relevant variable $\mathbf{P}$ instead of the full phase space $(\mathbf{q}, \mathbf{p})$. To this aim, a projector operator $\mathcal{P}$ is defined in the space of the observables

$$\mathcal{P}\mathbf{B} = \frac{\langle \mathbf{P}_0 \mathbf{B}_0 \rangle}{\langle \mathbf{P}_0{}^2 \rangle} \mathbf{P}_0, \tag{2}$$

where $\langle \cdot \rangle$ means an average over the stationary distribution corresponding to the evolution equation, Eq. (1). Together with the operator $\mathcal{Q} = 1 - \mathcal{P}$, the observable $\mathbf{B}$ can be decomposed into a contribution along the relevant variable $\mathbf{P}$ and another one orthogonal to it.

The Mori-Zwanzig theory is then based on Dyson's operator relation:[1]

$$e^{i\mathcal{L}t}\mathcal{Q} = \int_0^t e^{i\mathcal{L}(t-u)}\,\mathcal{P}i\mathcal{L}\,e^{i\mathcal{Q}\mathcal{L}u}\mathcal{Q}\,\mathrm{d}u + e^{i\mathcal{Q}\mathcal{L}t}\mathcal{Q}\,. \tag{3}$$

Noting that $e^{i\mathcal{L}t} = e^{i\mathcal{L}t}\mathcal{P} + e^{i\mathcal{L}t}\mathcal{Q}$, it is then possible to express the evolution of an observable $\mathbf{B}$ as

$$e^{i\mathcal{L}t}\mathbf{B} = e^{i\mathcal{L}t}\mathcal{P}\mathbf{B} + \int_0^t e^{i\mathcal{L}(t-u)}\,\mathcal{P}i\mathcal{L}\,e^{i\mathcal{Q}\mathcal{L}u}\mathcal{Q}\mathbf{B}\,\mathrm{d}u + e^{i\mathcal{Q}\mathcal{L}t}\mathcal{Q}\mathbf{B}\,. \tag{4}$$

Applying this relation to the rate of change of an observable $\mathbf{A}$, $\dot{\mathbf{A}}_t = i\mathcal{L}e^{i\mathcal{L}t}\mathbf{A}_0$, one obtains the GLE:

$$\dot{\mathbf{A}}_t = \frac{\mathrm{d}\mathbf{A}_t}{\mathrm{d}t} = i\Omega_A\mathbf{P}_t - \int_0^t K_A(u)\mathbf{P}_{t-u}\,\mathrm{d}u + \mathbf{R}_t\,, \tag{5}$$

with

$$i\Omega_A = \frac{\langle \mathbf{P}_0 \dot{\mathbf{A}}_0 \rangle}{\langle \mathbf{P}_0{}^2 \rangle}, \tag{6}$$

$$K_A(u) = \frac{\langle \dot{\mathbf{P}}_0\, e^{i\mathcal{Q}\mathcal{L}u}\mathcal{Q}\dot{\mathbf{A}}_0 \rangle}{\langle \mathbf{P}_0{}^2 \rangle} = \frac{\langle \dot{\mathbf{P}}_0\, \mathbf{R}_t \rangle}{\langle \mathbf{P}_0{}^2 \rangle}, \tag{7}$$

$$\mathbf{R}_t = e^{i\mathcal{Q}\mathcal{L}t}\mathcal{Q}\dot{\mathbf{A}}_0. \tag{8}$$

Equation (5) describes the dynamics of $\dot{\mathbf{A}}_t$ as the sum of a systematic and a random contribution. The systematic contribution is itself composed of a reversible term, Eq. (6), and retarded one involving the kernel, Eq. (7). Both depend only on the evolution of the relevant variable $\mathbf{P}$. The third term, Eq. (8), accounts for the effect of the other degrees of freedom, which have been projected out. This contraction of information renders the evolution of this term more difficult to apprehend and thus appears as fluctuating or "random."

As mentioned above, an efficient approach to the diffusion of a tagged particle in a fluid is to consider its momentum as both the relevant variable $\mathbf{P}$ and the observable $\mathbf{A}$. In that case the time-derivative of both quantities is the force acting on the particle and the denominator in Eqs. (6) and (7) is equal to mk_BT with m the mass of the particle, k_B Boltzmann's constant, and T the temperature. In addition, the reversible term Eq. (6) vanishes and the term defined by Eq. (8) is a random force. By analogy, we will refer in the following to $\mathbf{F} \equiv \dot{\mathbf{P}} = i\mathcal{L}\mathbf{P}$ as a force and to $\langle \mathbf{P}^2 \rangle$ as a kinetic energy even in the case of a generic variable. We note that in this case the memory kernel reduces to the auto-correlation function (ACF) of the random force, as will be discussed below.

One then usually assumes particular properties for this random term and the corresponding memory kernel. The most simple (and widespread) Markovian assumption, which becomes exact in the limit where the ratio between the mass of the considered solute and that of the bath molecules tends to infinity, considers a Gaussian distribution and a vanishing correlation time for the random force. This results in a memory kernel $K(u) = \gamma\delta(u)$, with δ the Dirac distribution and the friction $\gamma = \int_0^\infty K(u)\mathrm{d}u$. Long-time correlations due to the solvent backflow around the solute can be captured within the framework of continuous hydrodynamic theories, resulting in $K(u) \propto -u^{-3/2}$, which captures the resonances observed experimentally on colloidal particles.[6]

B. Projected correlation functions

The memory kernel $K_A(t)$, which determines the retarded contribution, involves the correlation function of the random term $\mathbf{R}$ and the derivative of the relevant variable $\dot{\mathbf{P}}$. It differs from a standard time-correlation function in that the dynamics entering the correlation function is not the normal dynamics generated by the Liouvillian $i\mathcal{L}$ but the one modified by the Mori projector and generated by $i\mathcal{Q}\mathcal{L}$.[8] Such *projected correlation functions* can be defined for any pair of observables $\mathbf{A}$ and $\mathbf{B}$ as

$$\bar{C}_{AB}(t) = \langle \mathbf{A}_0 e^{i\mathcal{Q}\mathcal{L}t}\mathbf{B}_0 \rangle\,, \tag{9}$$

but cannot be computed directly from the values of these observables along the trajectory. Note in particular that this definition depends not only on the two observables, but also on the choice of relevant variable $\mathbf{P}$ via the projector $\mathcal{Q}$. Since the operators $\mathcal{L}$, $\mathcal{P}$, and $\mathcal{Q}$ are hermitian for the scalar product $(\mathbf{C}, \mathbf{D}) = \langle \mathbf{C}\mathbf{D} \rangle$ of observables, the projected correlation function can also be rewritten as

$$\bar{C}_{AB}(t) = \langle (e^{-i\mathcal{L}\mathcal{Q}t}\mathbf{A}_0)\mathbf{B}_0 \rangle, \tag{10}$$

noting the inversion between $\mathcal{Q}$ and $\mathcal{L}$ in the propagator. We now discuss two approaches to extract projected correlation functions by adopting complementary points of view, corresponding to Eqs. (9) and (10), respectively. To that end, we first introduce $\mathbf{B}_t^+ \equiv e^{i\mathcal{Q}\mathcal{L}t}\mathbf{B}_0$, which propagates the observable $\mathbf{B}$ *forward* in time, during a time t, according to the

"orthogonal" dynamics generated by $i\mathcal{QL}$. This observable thus coincides with $\mathbf{B}$ at $t = 0$ and evolves according to

$$\frac{\mathrm{d}\mathbf{B}_t^+}{\mathrm{d}t} = i\mathcal{L}\mathbf{B}_t^+ - \mathcal{P}i\mathcal{L}\mathbf{B}_t^+ \,. \tag{11}$$

Similarly we define $\mathbf{A}_t^- \equiv e^{-i\mathcal{LQ}t}\mathbf{A}_0$, which propagates the observable $\mathbf{A}$ *backward* in time, during a time t, according to the "orthogonal" dynamics. It coincides with $\mathbf{A}$ at $t = 0$ and evolves according to

$$\frac{\mathrm{d}\mathbf{A}_t^-}{\mathrm{d}t} = -i\mathcal{L}\mathbf{A}_t^- + i\mathcal{LP}\mathbf{A}_t^- \,. \tag{12}$$

The projected correlation function $\bar{C}_{AB}(t)$ can then be written as two different, seemingly usual correlation functions:

$$\bar{C}_{AB}(t) = \langle \mathbf{A}_0\mathbf{B}_t^+\rangle = \langle \mathbf{A}_t^-\mathbf{B}_0\rangle \,. \tag{13}$$

In the following, we introduce two algorithms to compute $\bar{C}_{AB}(t)$ using these two expressions. We then discuss the properties of the random noise, before turning to results from molecular dynamics simulations.

C. Forward orthogonal dynamics, looking back

While Eq. (13) provides convenient expressions of $\bar{C}_{AB}(t)$ as a normal correlation function, the observables $\mathbf{B}_t^+$ and $\mathbf{A}_t^-$ evolve according to modified dynamics and cannot simply be measured at each time of the trajectory. We first describe an algorithm to compute the observable $\mathbf{B}_t^+$, which evolves according to the forward orthogonal dynamics, and thus projected correlation functions by Eq. (13). As shown in Appendix A, $\mathbf{B}_t^+$ satisfies

$$\mathbf{B}_t^+(\mathbf{q},\mathbf{p}) = \mathbf{B}_t(\mathbf{q},\mathbf{p}) + \int_0^t \mathbf{P}_{t-u}(\mathbf{q},\mathbf{p})\frac{\langle \mathbf{F}_0\mathbf{B}_u^+\rangle}{\langle \mathbf{P}_0^2\rangle}\mathrm{d}u \,. \tag{14}$$

We then write this expression at time $t + \delta t$ and separate the integral between 0 and t on the one hand, and between t and $t + \delta t$ on the other hand. Noting that for an observable $\mathbf{D}$ evolving under the normal dynamics, such as $\mathbf{P}$ or $\mathbf{B}$, we have by definition $\mathbf{D}_{t+\delta t}(\mathbf{q},\mathbf{p}) = \mathbf{D}_t(\mathbf{q}^{\delta t},\mathbf{p}^{\delta t})$, and finally making the change of variable $u \to u - t$ in the remaining integral, we obtain

$$\mathbf{B}_{t+\delta t}^+(\mathbf{q},\mathbf{p}) = \mathbf{B}_t^+(\mathbf{q}^{\delta t},\mathbf{p}^{\delta t}) + \int_0^{\delta t} \mathbf{P}_{-u}(\mathbf{q}^{\delta t},\mathbf{p}^{\delta t})\frac{\langle \mathbf{F}_0\mathbf{B}_{t+u}^+\rangle}{\langle \mathbf{P}_0^2\rangle}\mathrm{d}u \,. \tag{15}$$

In principle, several numerical schemes can be used to discretize the integral. The most simple, explicit form reads

$$\mathbf{B}_{t+\delta t}^+(\mathbf{q},\mathbf{p}) = \mathbf{B}_t^+(\mathbf{q}^{\delta t},\mathbf{p}^{\delta t}) + \mathbf{P}_0(\mathbf{q}^{\delta t},\mathbf{p}^{\delta t})\frac{\langle \mathbf{F}_0\mathbf{B}_t^+\rangle}{\langle \mathbf{P}_0^2\rangle}\delta t + \mathcal{O}(\delta t^2) \,. \tag{16}$$

This is easily implemented from a molecular dynamics trajectory of length N_{traj} steps as follows. The observables $\mathbf{A}$, $\mathbf{P}$, $\mathbf{F}$, and $\mathbf{B}_t^+$ are stored in four arrays

$$\begin{aligned} A_0(m) &\equiv \mathbf{A}_0(\mathbf{q}^{m\delta t},\mathbf{p}^{m\delta t}),\\ P_0(m) &\equiv \mathbf{P}_0(\mathbf{q}^{m\delta t},\mathbf{p}^{m\delta t}),\\ F_0(m) &\equiv \mathbf{F}_0(\mathbf{q}^{m\delta t},\mathbf{p}^{m\delta t}),\\ B_n^+(m) &\equiv \mathbf{B}_{n\delta t}^+(\mathbf{q}^{m\delta t},\mathbf{p}^{m\delta t}), \end{aligned} \tag{17}$$

with $m \in [0, N_{traj} - 1]$, δt the time step of the molecular dynamics, and initially $n = 0$. The first three contain the value of $\mathbf{A}$, $\mathbf{P}$, and $\mathbf{F}$ for each configuration along the whole trajectory and are never updated during the procedure. The last one evolves iteratively for $n \in [0, N_{corr} - 1]$ where N_{corr} is the length for which one wants to calculate the correlation, starting from the initial values $B_0^+(m) \equiv \mathbf{B}_0(\mathbf{q}^{m\delta t},\mathbf{p}^{m\delta t})$, according to

$$B_{n+1}^+(m) = B_n^+(m+1) + \beta(n)P_0(m+1)\delta t \,, \tag{18}$$

with

$$\beta(n) = \frac{\sum_{m=0}^{N_{traj}-n-1} F_0(m)B_n^+(m)}{\sum_{m=0}^{N-n-1} P_0(m)^2} \,. \tag{19}$$

This allows to reconstruct the evolution of $\mathbf{B}_t^+$ from each configuration along the trajectory and to analyze its properties. In particular, the kernel $\bar{C}_{AB}$ is calculated for $t = n\delta t$ from Eq. (13) as the scalar product of the arrays A_0 and B_n^+:

$$C_{AB}(n\delta t) = \frac{1}{N_{traj} - n}\sum_{m=0}^{N_{traj}-n-1} A_0(m)B_n^+(m) \,. \tag{20}$$

As mentioned above, in the case where $\mathbf{P}$ is the momentum of a tagged particle, $\mathbf{F}$ is the force acting on it, and $\langle \mathbf{P}^2\rangle$ is proportional to the thermal energy. This average can then be computed with a better accuracy using the instantaneous kinetic energy in the interval $m \in [0, N_{traj} - n - 1]$ instead of the average temperature over the whole trajectory. We named this algorithm according to the fact that we correlate the observable $\mathbf{B}_t^+$, evolved forward in time according to the orthogonal dynamics $i\mathcal{QL}$ from an initial condition, with the observable $\mathbf{A}$ at the initial time, i.e., looking back. This algorithm requires $\mathcal{O}(N_{traj})$ of memory size and the calculation time is $\mathcal{O}(N_{traj}N_{corr})$.

D. Backward orthogonal dynamics, looking ahead

In this second approach, we introduce an auxiliary operator $\tilde{\mathbf{A}}_t^- = e^{i\mathcal{L}t}\mathbf{A}_t^-$, which coincides with $\mathbf{A}$ at $t = 0$ and evolves as (see Appendix B):

$$\frac{\mathrm{d}\tilde{\mathbf{A}}_t^-}{\mathrm{d}t} = (-i\mathcal{L})\,\mathcal{P}_t\tilde{\mathbf{A}}_t^- \,, \tag{21}$$

where we have defined a time-dependent projection operator $\mathcal{P}_\tau = e^{i\mathcal{L}\tau}(\mathcal{P})e^{-i\mathcal{L}\tau}$, which is the projection on the relevant variable $\mathbf{P}$ at time τ. The projected correlation function is then

$$\bar{C}_{AB}(t) = \langle \tilde{\mathbf{A}}_t^-(\mathbf{q},\mathbf{p})\mathbf{B}_0(\mathbf{q}^t,\mathbf{p}^t)\rangle = \langle \tilde{\mathbf{A}}_t^-\mathbf{B}_t\rangle \,, \tag{22}$$

i.e., the correlation function between $\tilde{\mathbf{A}}_t^-$ and $\mathbf{B}$ at a time t *forward* in time. The value of $\tilde{\mathbf{A}}_t^-$ at the phase space point

$(\mathbf{q}, \mathbf{p})$ is however updated according to

$$\frac{\mathrm{d}\tilde{\mathbf{A}}_t^-(\mathbf{q},\mathbf{p})}{\mathrm{d}t} = \frac{\langle \mathbf{P}_t \tilde{\mathbf{A}}_t^- \rangle}{\langle \mathbf{P}_0{}^2 \rangle} \mathbf{F}_t(\mathbf{q},\mathbf{p}). \tag{23}$$

The structure of these equations allows for the computation of the projected correlation function on-the-fly, contrary to the previous method which requires generating the trajectory as a prior step. We first choose the number of consecutive steps N_{av} used to compute the averages. At each time step $t = n\delta t$ along the dynamics, we consider again four arrays,

$$\begin{aligned} \tilde{A}_n^-(m) &\equiv \tilde{\mathbf{A}}_{n\delta t}^-(\mathbf{q}^{m\delta t}, \mathbf{p}^{m\delta t}), \\ P_n(m) &\equiv \mathbf{P}_0(\mathbf{q}^{m\delta t+n\delta t}, \mathbf{p}^{m\delta t+n\delta t}), \\ F_n(m) &\equiv \mathbf{F}_0(\mathbf{q}^{m\delta t+n\delta t}, \mathbf{p}^{m\delta t+n\delta t}), \\ B_n(m) &\equiv \mathbf{B}_0(\mathbf{q}^{m\delta t+n\delta t}, \mathbf{p}^{m\delta t+n\delta t}), \end{aligned} \tag{24}$$

for $m \in [0, N_{av} - 1]$. Note the offset $n\delta t$ in the three arrays $P_n(m)$, $F_n(m)$, and $B_n(m)$. The first initial N_{av} steps of the trajectory are used to initialize these arrays for $t = 0$, using for $\tilde{A}_0^-(m)$ the instantaneous observable $\mathbf{A}_0(\mathbf{q}^{m\delta t}, \mathbf{p}^{m\delta t})$. Then at each time step $t = n\delta t$, the scalar product between $\tilde{A}_n^-(m)$ and $B_n(m)$ allows computing the projected correlation function as

$$\bar{C}_{AB}(t) = \frac{1}{N_{av}} \sum_{m=0}^{N_{av}-1} \tilde{A}_n^-(m) \times B_n(m). \tag{25}$$

Upon evolution from t to $t + \delta t$, the arrays $P_n(m)$, $F_n(m)$, and $B_n(m)$ are appended by the instantaneous value of the property (e.g., momentum), of its time derivative (e.g., force) and of the observable B for the new configuration, while the oldest configuration is discarded. These arrays then contain the values of $\mathbf{P}$ and $\dot{\mathbf{P}}$ from time $t + \delta t$ to $t + N_{av}\delta t$. The array $\tilde{A}_n^-$, which would be left untouched when computing a standard correlation function, is updated according to

$$\tilde{A}_{n+1}^-(m) = \tilde{A}_n^-(m) + \alpha(n) F_n(m) \delta t \ , \tag{26}$$

for $m \in [0, N_{av} - 1]$, with

$$\alpha(n) = \frac{\sum_{m=0}^{N_{av}-1} \tilde{A}_n^-(m) P_n(m)}{\sum_{m=0}^{N_{av}-1} P_n(m)^2}. \tag{27}$$

As with the previous method, in the case where $\mathbf{P}$ is the momentum of a tagged particle, $\mathbf{F}$ is the force acting on it and $\langle \mathbf{P}^2 \rangle$ is proportional to the thermal energy, and the numerical accuracy is increased by computing this average from the instantaneous kinetic energy in the interval $m \in [0, N_{av}]$ instead of the average temperature over the whole trajectory. Contrary to the usual procedure to compute time correlation functions, the timespan used for performing the average, N_{av} is pre-determined and running longer the simulation allows to evaluate the correlation function at longer times but not to increase the statistics. We circumvent this by calculating the projected correlation function per blocks of the simulation. This algorithm requires $\mathcal{O}(N_{av})$ of memory size and the calculation time is $\mathcal{O}(N_{av} N_{corr})$.

E. Statistical properties of the noise

1. Random noise, projected force, and memory kernel

Let us now consider a particular choice of observable $\mathbf{A}$ as the relevant variable $\mathbf{P}$. Its rate of change is then the force $\mathbf{F} = \dot{\mathbf{P}}$, given by the GLE, Eq. (5). Since in that case $\mathcal{Q}\mathbf{F} = \mathbf{F}$, the random force $\mathbf{R}_t = e^{i\mathcal{Q}\mathcal{L}t}\mathcal{Q}\mathbf{F}_0$ is equal to the observable $\mathbf{F}_t^+ = e^{i\mathcal{Q}\mathcal{L}t}\mathbf{F}_0$ and can thus be computed using the algorithm described above in the *forward orthogonal dynamics – looking back* scheme. It is then possible to test numerically some formal properties of the random force. In particular, since initially $\mathbf{R}_0 = \mathbf{F}_0^+ = \mathbf{F}_0$, the memory kernel defined by Eq. (7) and entering the GLE (5) is equal to the auto-correlation function of the random force: This is a form of the fluctuation-dissipation theorem. The above discussion and the introduction of the auxiliary observable $\mathbf{F}_t^+$ allow us to compute explicitly the random force and its auto-correlation function as

$$K_P(t) = \frac{\langle \mathbf{F}_0^+ \mathbf{F}_t^+ \rangle}{\langle \mathbf{P}_0^2 \rangle}. \tag{28}$$

We can further directly test other properties of this function. An important one is its stationarity, which does not follow immediately from the stationarity of the dynamics, since the evolution of the random force is not generated by the Liouvillian and since $\mathbf{F}_t^+$ is evolved from the initial condition $\mathbf{F}_0$ at a finite time t in the past. The stationarity of the noise auto-correlation function can be demonstrated as follows. We start from the definition of the projected force $\langle \mathbf{F}_0^+ \mathbf{F}_t^+ \rangle = \langle \mathcal{Q}\mathbf{F}_0 e^{i\mathcal{Q}\mathcal{L}t} \mathcal{Q}\mathbf{F}_0 \rangle$ and rewrite $e^{i\mathcal{Q}\mathcal{L}t}\mathcal{Q} = e^{-i\mathcal{Q}\mathcal{L}u}\mathcal{Q}e^{i\mathcal{Q}\mathcal{L}(t+u)}\mathcal{Q}$. Noting that $e^{-i\mathcal{Q}\mathcal{L}u}\mathcal{Q}$ is the adjoint of $e^{i\mathcal{Q}\mathcal{L}u}\mathcal{Q}$, we obtain

$$\begin{aligned} \langle \mathbf{F}_0^+ \mathbf{F}_t^+ \rangle &= \langle \mathcal{Q}\mathbf{F}_0 e^{-i\mathcal{Q}\mathcal{L}u} \mathcal{Q} e^{i\mathcal{Q}\mathcal{L}(t+u)} \mathcal{Q}\mathbf{F}_0 \rangle \\ &= \langle e^{i\mathcal{Q}\mathcal{L}u} \mathcal{Q}\mathbf{F}_0 e^{i\mathcal{Q}\mathcal{L}(t+u)} \mathcal{Q}\mathbf{F}_0 \rangle \\ &= \langle \mathbf{F}_u^+ \mathbf{F}_{t+u}^+ \rangle \ , \end{aligned} \tag{29}$$

where we have also used the fact that $\mathcal{Q}^2 = \mathcal{Q}$.

2. Markovian approximation and Einstein relation

Choosing again $\mathbf{A}$ as the relevant variable $\mathbf{P}$, we now consider the case where the memory kernel decays very fast compared to the time scale of interest. The GLE (5) then simplifies to

$$\dot{\mathbf{P}}_t = -\gamma \mathbf{P}_t + \mathbf{R}_t \ , \tag{30}$$

where we introduced the friction coefficient:

$$\gamma = \int_0^\infty K_P(t)\,\mathrm{d}t = \int_0^\infty \frac{\langle \mathbf{F}_0^+ \mathbf{F}_t^+ \rangle}{\langle \mathbf{P}_0^2 \rangle}\,\mathrm{d}t \ . \tag{31}$$

In the case where the relevant variable is the momentum of a tagged particle, Einstein's relation states that the friction γ is related to the diffusion coefficient as $\gamma = k_B T/mD$. Expressions analogous to the Einstein relation can be obtained for generic observables $\mathbf{P}$, even though the quantities to which the friction are related are not as simple as the diffusion coefficient.

3. Velocity, force, and noise distributions

Limiting again ourselves to the case of the momentum of a tagged particle as the relevant variable $\mathbf{P}$, the equilibrium distribution of the velocity arising form both the microscopic dynamics and the GLE should be Gaussian with a variance $\langle \mathbf{P_0}^2 \rangle = mk_BT$ (Maxwell distribution). In the Markovian limit, the noise also follows a Gaussian distribution with a variance $\langle \mathbf{R_0}^2 \rangle = m\gamma k_BT$. In general, however, this is not the case. In particular, the finite- or long-time decay may result in fat tails in the distribution of the force and the noise, while the velocities should follow the same Maxwell distribution. It follows from the GLE, Eq. (5), that the difference $\dot{\mathbf{P}}_t - \mathbf{R}_t$ between the force and the noise is the sum only of terms involving the velocity, hence follows a Gaussian distribution. This suggests that this difference may also be Gaussian distributed in general, as it is obviously in the Markovian limit since this difference is then simply $-\gamma \mathbf{P}_t$, see Eq. (30).

III. SIMULATION RESULTS

A. Numerical details

Since the most standard application of the Mori-Zwanzig formalism considers the velocity or momentum of a tagged particle in a fluid as the relevant variable, we have chosen to illustrate the two algorithms on this particular case. More precisely, we consider a LJ fluid at a reduced density $\rho^* = \rho\sigma^3 = 0.5$, with σ the LJ diameter, and reduced temperature $T^* = k_BT/\epsilon = 1.5$, with ϵ the LJ energy. The simulated system consists of 10^3 LJ particles in a cubic box of length 12.6σ, with periodic boundary conditions in all directions. Interactions are computed using a cut-off radius $r_c = 6\sigma$. Newton's equations of motion are solved using the Leap-Frog Verlet algorithm with a time-step $10^{-3}t^*$ where $t^* = \sqrt{m\sigma^2/\epsilon}$, with m the mass of the LJ particles. The system is first equilibrated at the target temperature during $10t^*$ by performing molecular dynamics in the NVT ensemble using the Nosé-Hoover thermostat with a time constant of $10^{-3}t^*$. All properties are then determined from a $10t^*$ trajectory in the NVE ensemble. We consider first the usual case where both observables $\mathbf{A}$ and $\mathbf{B}$ are taken as the force acting on the tagged particle. We then illustrate how the present algorithms can be used on a different choice of observables.

The *forward orthogonal dynamics, looking back* algorithm can be applied *a posteriori* to a trajectory generated by any simulation package, provided that it allows the computation of the quantities described by Eq. (17). The results described below were obtained from trajectories generated with the DL_POLY simulation package.[17] A specific program was written to compute the random force and the memory kernel. In order to accurately integrate Eqs. (11) and (12) to obtain the random force and the corresponding memory kernel, in particular at long times, it is important not to sub-sample the trajectory and to use the momentum and force at each time step.

The *backward orthogonal dynamics, looking ahead* only requires data from previous time steps and can thus be implemented on-the-fly. To that end, we have written a specific molecular dynamics code. A Verlet list was used to compute interactions, with a skin at $1.1r_c$ and updated every 50 steps. We have chosen $N_{av} = 4000$ for the averaging needed for the projection (see Sec. II D), and the time-correlation was calculated up to $t_{max} = t^*$, i.e., 1000 steps. The projected correlation functions are thus calculated from 5000 time-step trajectories. For improving the statistics, we have further averaged the projected correlations over four successive blocks so that the total length of the trajectory is $N = 2 \times 10^4$ steps.

B. Autocorrelation functions

Before discussing the properties of the velocity, force, and noise ACF, we first investigate the predictions of both algorithms for the noise ACF. Figure 1 compares the noise ACF $\bar{C}_{FF}(t) = \langle \mathbf{F}_0\mathbf{F}_t^+ \rangle$ obtained by both algorithms to that obtained from usual correlation functions using Laplace transforms.[13] In practice, a numerically stable evaluation can be obtained from the Laplace transforms ($\mathcal{LT}$) of the velocity ACF $C_{vv}(t) = \langle \mathbf{v}_0\mathbf{v}_t \rangle$ and the force-velocity cross-correlation function $C_{vF}(t) = \langle \mathbf{v}_0\mathbf{F}_t \rangle$ as

$$\bar{C}_{FF}(t) = \mathcal{LT}^{-1}\left(\frac{\mathcal{LT}[C_{vF}]}{\mathcal{LT}[C_{vv}]}\right). \tag{32}$$

The agreement between the three methods is excellent. This validates the two algorithms introduced in the present work for this particular choice of observables. The Laplace route only provides the autocorrelation of the noise. By contrast, the methodologies introduced here give direct access to the projected quantities $\mathbf{B}_t^+(\mathbf{q}, \mathbf{p})$ and $\mathbf{A}_t^-(\mathbf{q}, \mathbf{p})$, allowing for the study of their properties or the calculation of generic projected correlation functions where $\mathbf{A}$ or $\mathbf{B}$ are not the force $\mathbf{F}$.

Figure 2 compares the force autocorrelation function (FACF) to the random noise auto-correlation function (NACF), which is the memory kernel. As expected, the NACF decorrelates faster than the FACF, even though both coincide at very short times. The longer decorrelation time seen in the negative part of the FACF is due to the feedback of the environment on the tagged particle. This systematic feedback is also at the origin of the power law decay of the velocity autocorrelation function (VACF), also shown here, but does not enter in the random noise. Since they are based on the Mori-Zwanzig approach, the algorithms presented here allow

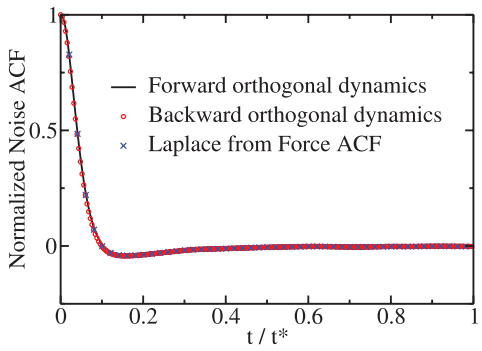

FIG. 1. Noise auto-correlation function, obtained from molecular dynamics using the *forward orthogonal dynamics, looking back* (black line) and *backward orthogonal dynamics, looking ahead* (red circles) algorithms and from the force autocorrelation function using Laplace transforms (blue crosses).

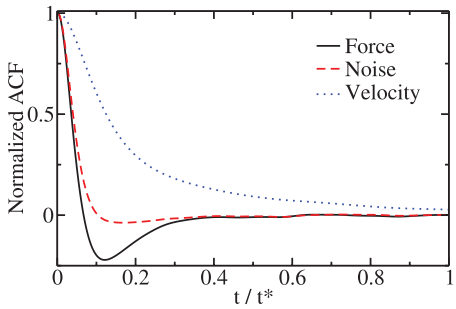

FIG. 2. Auto-correlation functions: force (solid black line), noise (dashed red line), and velocity (dotted blue line).

to disentangle the systematic and random forces in the effect of the environment. At this point, it is interesting to see that also the NACF exhibits one oscillation. A similar behaviour has been found in a recent single particle experiment.[6] A major difference between the FACF and the NACF is that the former integrates to zero while the latter integrates to the friction ($\gamma \approx 5.2$ LJ units in the present case) which enters the simple Langevin equation (30) in the Markovian limit.

C. Statistical properties of the random force

Using the *forward orthogonal dynamics, looking back* algorithm, it is possible to reconstruct, from each point along the trajectory, the projected force $\mathbf{F}^+$ for the subsequent times. This allows us to examine numerically several properties of this noise history.

1. Check of stationarity

The noise is the result of the propagation by $\mathcal{QL}$ of the normal force from time 0 to time t. From Eq. (28), the memory kernel is computed by correlating the noise after a delay t from each starting point ($\langle \mathbf{F}_0^+ \mathbf{F}_t^+ \rangle$). It can also be computed by correlating the noise after a delay u and a delay $t+u$ from each starting point ($\langle \mathbf{F}_u^+ \mathbf{F}_{t+u}^+ \rangle$), as a result of the stationarity demonstrated in Eq. (29). Figure 3 compares the results of molecular simulations for two waiting times u. This figure clearly demonstrates that the computed noise auto-correlation function satisfies the stationarity condition. It is a numerical test of the stationarity and also indicates that the algorithm proposed is quite stable.

2. Velocity, force, and noise distributions

Exploiting further the possibilities offered by the reconstruction of the projected force with the *forward orthogonal dynamics, looking back* method, we now analyze the distribution of the noise history from a single initial condition. Figure 4 reports this distribution, together with the velocity and force distribution and that of the difference $\dot{\mathbf{P}}_t - \mathbf{R}_t$ between force and noise. While the velocity distribution is Gaussian (Maxwell distribution), with the expected variance k_BT/m, the force and noise are markedly non-Gaussian, with fat tails. A similar observation had been made by Shin *et al.* for a two-dimensional fluid.[13]

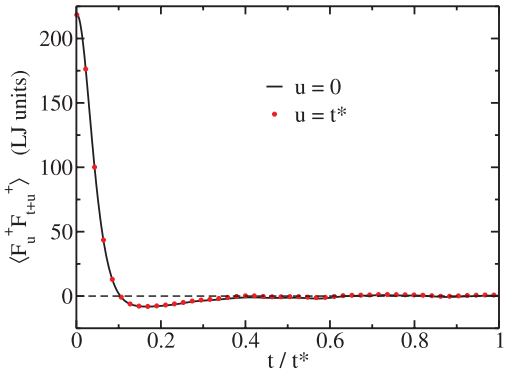

FIG. 3. Each configuration along the trajectory can be used as the starting point for the reconstruction of the projected force (noise). The noise ACF is straightforwardly computed by correlating the noise after a delay t from each starting point ($\langle \mathbf{F}_0^+ \mathbf{F}_t^+ \rangle$). It can also be computed by correlating the noise after a delay u and a delay $t+u$ from each starting point ($\langle \mathbf{F}_u^+ \mathbf{F}_{t+u}^+ \rangle$). The results from molecular simulation, illustrated here for $u = 0$ (line) and $u = t^*$ (symbols), demonstrate the stationarity of the NACF, which is not an obvious property – see Eq. (29).

Interestingly, while both the force and noise display fat tails, their difference is Gaussian, with a variance of ≈53 LJ units. As explained in Sec. II E 3, the difference is the sum of a large number of terms drawn from the Gaussian velocity distribution. In the Markovian limit, it is clear from Eq. (30) that the variance of this distribution should be $\gamma^2 m k_B T$, i.e., ≈41 LJ units in the present case. This suggests that this approximation may be reasonable in that case.

D. Other observables: Short- and long-range forces

The methodology developed here further allows us to estimate projected correlation functions not only for the force, i.e., the NACF, but also for any pair of observables. We illustrate this ability on a particular choice of observables, in order to gain insight into the origin of the time-dependence of the NACF. More precisely, since momentum transfer inside the fluid arises primarily from the short-range repulsion between

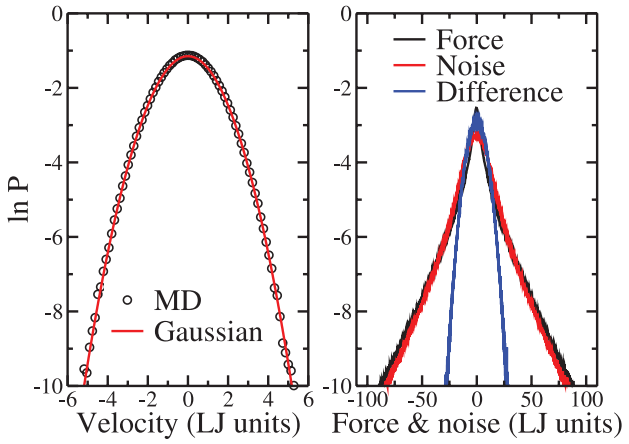

FIG. 4. Left panel: The velocity of the particles follows the Gaussian Maxwell distribution (note the logarithmic scale for the probability P). Right panel: The force and noise distributions are markedly non-Gaussian, with fat tails. The distribution of their difference, which corresponds to the memory term, does not display such fat tails and is almost Gaussian.

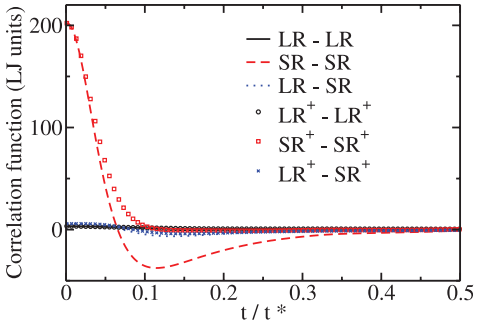

FIG. 5. Auto- and cross-correlation functions for the long (LR) and short (SR) range contributions to the force (lines), defined by Eq. (33), and of the corresponding projected forces (symbols).

particles (which also dictates the structure),[18] we choose as observables the short range repulsive (SR) and long range attractive (LR) parts of the Lennard-Jones potential according to the Weeks-Chandler-Andersen prescription, i.e.:

$$\begin{aligned} V_{\mathrm{SR}}(r) &= V_{\mathrm{LJ}}(r) + \epsilon \text{ for } r \leq \sigma\ ,\ 0 \text{ otherwise,} \\ V_{\mathrm{LR}}(r) &= V_{\mathrm{LJ}}(r) \text{ for } r \geq \sigma\ ,\ -\epsilon \text{ otherwise.} \end{aligned} \tag{33}$$

We have applied the two procedures introduced here to the evolution of the forces corresponding to both contributions according to the projected dynamics and computed the associated auto- and cross-correlation functions.

The different contributions are shown in Figure 5. It appears that the NACF is completely dominated by the short-range collisions. In addition, the dynamics of this projected short-range force coincides with the short-range force only at short times ($t \lesssim 0.05t^*$). As for the total force, the NACF barely becomes negative at intermediate times, while the FACF does. The long-range ACF and the cross-correlation function do not display such large differences between the dynamics of the normal and projected quantities.

We can further analyze relative contributions of the short- and long-range projected forces to the friction given by Eq. (31) in the Markovian limit. The integrals of the correlation functions of Figure 5 are reported in Figure 6. For the long-range part, the normal and projected dynamics almost coincide, so that the corresponding correlation functions integrate to

$$\int_0^\infty \frac{\langle \mathbf{F}_{LR,0}\mathbf{F}_{LR,t}\rangle}{\langle \mathbf{P}_0^2\rangle}\,\mathrm{d}t \approx \int_0^\infty \frac{\langle \mathbf{F}^+_{LR,0}\mathbf{F}^+_{LR,t}\rangle}{\langle \mathbf{P}_0^2\rangle}\,\mathrm{d}t = \gamma_{LL}\ . \tag{34}$$

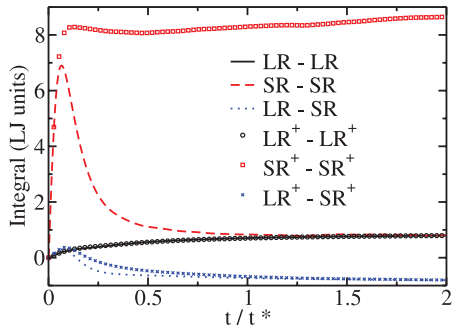

FIG. 6. Integral of the correlation functions of Figure 5.

Similarly, we find that

$$\int_0^\infty \frac{\langle \mathbf{F}_{LR,0}\mathbf{F}_{SR,t}\rangle}{\langle \mathbf{P}_0^2\rangle}\,\mathrm{d}t \approx \int_0^\infty \frac{\langle \mathbf{F}^+_{LR,0}\mathbf{F}^+_{SR,t}\rangle}{\langle \mathbf{P}_0^2\rangle}\,\mathrm{d}t = \gamma_{LS}\ . \tag{35}$$

In addition, we find that γ_{LS} and γ_{LL} are opposite. Finally, the ACF for the short-range part is equal to γ_{LL} for the non-projected forces but is much larger in the projected case, due to the lack of negative part in the ACF. These observations are consistent with the fact that the integral of the ACF for the total force $\mathbf{F}_{SR} + \mathbf{F}_{LR}$ should vanish (since $\int_0^\infty \langle \mathbf{F}_0\mathbf{F}_t\rangle\,\mathrm{d}t = -\langle \mathbf{F}_0\mathbf{P}_0\rangle = 0$). The total friction $\gamma = \gamma_{LL} + \gamma_{SS} + 2\gamma_{LS}$ is then completely dominated by γ_{SS}, i.e., the short-range autocorrelation. As a final remark, we note that the diffusion coefficient obtained from $D = \int_0^\infty C_{vv}(t)\,\mathrm{d}t \approx 0.33$ LJ units is in good agreement with that predicted by the Einstein relation, $k_BT/m\gamma \approx 0.29$ LJ units.

IV. CONCLUSION

We have developed two original algorithms for the computation of projected correlation functions for any pair of observables. These algorithms are based on a suitable propagation of the observables measured at given phase space points. One algorithm, denoted *Forward orthogonal dynamics, looking back*, is based on the forward orthogonal dynamics. It needs the whole trajectory to be known in advance and is thus implemented outside the MD simulation itself. The second algorithm, *Backward orthogonal dynamics, looking ahead*, uses a propagation of the observables backward according to the adjoint of the orthogonal dynamics. Although the adjoint dynamics is less natural, it can be implemented alongside the MD simulation.

As a test application, the motion of a tagged particle in a LJ fluid, the two algorithms were shown to give identical results and to be quite stable. The algorithm *Forward orthogonal dynamics, looking back* also allowed us to extract the random force, or noise, in order to study its properties. The computed random force then showed a clear non-Gaussian statistics. Finally, since the algorithms can be used to propagate any observable according to the orthogonal dynamics, it was possible to separate the long range and short range contributions to the Langevin kernel describing the motion of the tagged particle in a LJ fluid. We showed that the short-range/short-range term is the major contribution to the overall friction, although the other terms are not fully negligible. The short-range/short-range force correlation function is also the most affected by going from the normal correlation function to the projected correlation function.

The proposed algorithms thus pave the way for the analysis of the origin of the friction kernel and the total friction exerted on the relevant degrees of freedom. For example, it may be used to study the effect of confinement and the different roles of the solvent and the confining material. We have recently applied it to the case of ions confined in clay minerals.[19] It also allows to straightforwardly study projected correlation functions that are not simply force-force correlation functions for describing the non-instantaneous response to the dynamics of the relevant degrees of freedom, as, for

example, the non-local response of the surrounding to the motion of a Brownian particle.[20,21] We are currently investigating the long-time behaviour of the memory kernel in order to assess the relevance of the usual approximations. Overall, these algorithms provide a new tool to bridge the gap between fully atomistic models and effective dynamics described by generalized Langevin equations.

ACKNOWLEDGMENTS

A.C. acknowledges financial support from the Ecole Normale Supérieure.

APPENDIX A: EVOLUTION OF $\mathbf{B}_t^+$

In order to compute the projected correlation function $\bar{C}_{AB}(t)$ between two observables $\mathbf{A}$ and $\mathbf{B}$, we introduce the auxiliary observable $\tilde{\mathbf{B}}_t^+ = e^{-i\mathcal{L}t}\mathbf{B}_t^+ = e^{-i\mathcal{L}t}e^{i\mathcal{Q}\mathcal{L}t}\mathbf{B}_0$. The definition (9) of $\bar{C}_{AB}(t)$ can then be rewritten using $\mathbf{B}_t^+$ as Eq. (13) or with $\tilde{\mathbf{B}}_t^+$, making explicit the space point $(\mathbf{q}, \mathbf{p})$ on which the operators apply, as

$$\begin{aligned}\bar{C}_{AB}(t) &= \langle \mathbf{A}_0(\mathbf{q},\mathbf{p})(e^{i\mathcal{L}t}\tilde{\mathbf{B}}_t^+)(\mathbf{q},\mathbf{p})\rangle \\ &= \langle \mathbf{A}_0(\mathbf{q},\mathbf{p})\tilde{\mathbf{B}}_t^+(\mathbf{q}^t,\mathbf{p}^t)\rangle \\ &= \langle (e^{-i\mathcal{L}t}\mathbf{A}_0)(\mathbf{q},\mathbf{p})\tilde{\mathbf{B}}_t^+(\mathbf{q},\mathbf{p})\rangle \\ &= \langle \mathbf{A}_0(\mathbf{q}^{-t},\mathbf{p}^{-t})\tilde{\mathbf{B}}_t^+(\mathbf{q},\mathbf{p})\rangle \ , \end{aligned} \tag{A1}$$

recalling that $(\mathbf{q}^t, \mathbf{p}^t)$ is the space point at time t from the initial space point $(\mathbf{q}, \mathbf{p})$. From its definition and Eq. (11), it follows that the operator $\tilde{\mathbf{B}}_t^+$ evolves as

$$\begin{aligned}\frac{\mathrm{d}\tilde{\mathbf{B}}_t^+(\mathbf{q},\mathbf{p})}{\mathrm{d}t} &= -i\mathcal{L}e^{-i\mathcal{L}t}\mathbf{B}_t^+ + e^{-i\mathcal{L}t}i\mathcal{Q}\mathcal{L}\mathbf{B}_t^+ \\ &= e^{-i\mathcal{L}t}(-i\mathcal{L}+i\mathcal{Q}\mathcal{L})\mathbf{B}_t^+ = e^{-i\mathcal{L}t}\mathcal{P}(-i\mathcal{L})e^{i\mathcal{L}t}\tilde{\mathbf{B}}_t^+ \\ &= \mathcal{P}_{-t}(-i\mathcal{L})\tilde{\mathbf{B}}_t^+(\mathbf{q},\mathbf{p}) \ , \end{aligned} \tag{A2}$$

where we have also used the fact that $i\mathcal{L}$ commutes with $e^{\pm i\mathcal{L}t}$ and where $\mathcal{P}_\tau = e^{i\mathcal{L}\tau}(\mathcal{P})e^{-i\mathcal{L}\tau}$ is the projection on the relevant variable $\mathbf{P}$ at time τ. This can be shown by considering the action of $\mathcal{P}_\tau$ on an observable $\mathbf{C}$ as

$$\begin{aligned}\mathcal{P}_\tau\mathbf{C}(\mathbf{q},\mathbf{p}) &= e^{i\mathcal{L}\tau}\mathbf{P}_0(\mathbf{q},\mathbf{p})\frac{\langle \mathbf{P}_0(e^{-i\mathcal{L}\tau}\mathbf{C})\rangle}{\langle \mathbf{P}_0^2\rangle} \\ &= (e^{i\mathcal{L}\tau}\mathbf{P}_0)(\mathbf{q},\mathbf{p})\frac{\langle (e^{i\mathcal{L}\tau}\mathbf{P}_0)\mathbf{C}\rangle}{\langle \mathbf{P}_0^2\rangle} \ , \end{aligned} \tag{A3}$$

and by remembering that $(e^{i\mathcal{L}\tau}\mathbf{P}_0)(\mathbf{q},\mathbf{p}) = \mathbf{P}_0(\mathbf{q}^\tau,\mathbf{p}^\tau) = \mathbf{P}_\tau(\mathbf{q},\mathbf{p})$. Since in addition $\langle \mathbf{P}(-i\mathcal{L})\mathbf{C}\rangle = \langle (i\mathcal{L})\mathbf{P}\mathbf{C}\rangle = \langle \mathbf{F}\mathbf{C}\rangle$, it follows that

$$\mathcal{P}_{-t}(-i\mathcal{L})\mathbf{C}(\mathbf{q},\mathbf{p}) = \mathbf{P}_{-t}(\mathbf{q},\mathbf{p})\frac{\langle \mathbf{F}_{-t}\mathbf{C}\rangle}{\langle \mathbf{P}_0^2\rangle} \ . \tag{A4}$$

Applying this to $\mathbf{C}(\mathbf{q},\mathbf{p}) = \tilde{\mathbf{B}}_t^+(\mathbf{q},\mathbf{p})$, Eq. (A2) can be formally integrated from $\tilde{\mathbf{B}}_0^+(\mathbf{q},\mathbf{p}) = \mathbf{B}_0^+(\mathbf{q},\mathbf{p}) = \mathbf{B}_0(\mathbf{q},\mathbf{p})$ to obtain

$$\tilde{\mathbf{B}}_t^+(\mathbf{q},\mathbf{p}) = \mathbf{B}_0(\mathbf{q},\mathbf{p}) + \int_0^t \mathbf{P}_{-u}(\mathbf{q},\mathbf{p})\frac{\langle \mathbf{F}_{-u}\tilde{\mathbf{B}}_u^+\rangle}{\langle \mathbf{P}_0^2\rangle}\mathrm{d}u \ . \tag{A5}$$

This can be rewritten, using $\mathbf{B}_t^+ = e^{i\mathcal{L}t}\tilde{\mathbf{B}}_t^+$ and the fact that $\langle \mathbf{F}_{-u}\tilde{\mathbf{B}}_u^+\rangle = \langle \mathbf{F}_0\mathbf{B}_u^+\rangle$, as

$$\mathbf{B}_t^+(\mathbf{q},\mathbf{p}) = \mathbf{B}_t(\mathbf{q},\mathbf{p}) + \int_0^t \mathbf{P}_{t-u}(\mathbf{q},\mathbf{p})\frac{\langle \mathbf{F}_0\mathbf{B}_u^+\rangle}{\langle \mathbf{P}_0^2\rangle}\mathrm{d}u \ . \tag{A6}$$

Finally, making the change of variable $u \to t-u$ in the integral, we obtain

$$\mathbf{B}_t^+(\mathbf{q},\mathbf{p}) = \mathbf{B}_t(\mathbf{q},\mathbf{p}) + \int_0^t \mathbf{P}_u(\mathbf{q},\mathbf{p})\frac{\langle \mathbf{F}_0\mathbf{B}_{t-u}^+\rangle}{\langle \mathbf{P}_0^2\rangle}\mathrm{d}u \ . \tag{A7}$$

APPENDIX B: EVOLUTION OF $\mathbf{A}_t^-$

Similarly, the definition (9) of $\bar{C}_{AB}(t)$ can be rewritten using $\mathbf{A}_t^-$ as Eq. (13) or, using the stationarity of the probability density and the conservation of phase space volume:

$$\bar{C}_{AB}(t) = \langle \mathbf{A}_t^-(\mathbf{q}^t,\mathbf{p}^t)\mathbf{B}_0(\mathbf{q}^t,\mathbf{p}^t)\rangle \ . \tag{B1}$$

Introducing now the auxiliary observable $\tilde{\mathbf{A}}_t^- = e^{i\mathcal{L}t}\mathbf{A}_t^- = e^{i\mathcal{L}t}e^{-i\mathcal{L}\mathcal{Q}t}\mathbf{A}_0$, the projected correlation function reads

$$\bar{C}_{AB}(t) = \langle \tilde{\mathbf{A}}_t^-(\mathbf{q},\mathbf{p})\mathbf{B}_0(\mathbf{q}^t,\mathbf{p}^t)\rangle \ . \tag{B2}$$

From its definition and Eq. (12), it follows that the operator $\tilde{\mathbf{A}}_t^-$ evolves as

$$\begin{aligned}\frac{\mathrm{d}\tilde{\mathbf{A}}_t^-(\mathbf{q},\mathbf{p})}{\mathrm{d}t} &= i\mathcal{L}e^{i\mathcal{L}t}\mathbf{A}_t^- + e^{i\mathcal{L}t}(-i\mathcal{L}\mathcal{Q})\mathbf{A}_t^- \\ &= e^{i\mathcal{L}t}(i\mathcal{L}-i\mathcal{L}\mathcal{Q})\mathbf{A}_t^- = e^{i\mathcal{L}t}(i\mathcal{L}\mathcal{P})e^{-i\mathcal{L}t}\tilde{\mathbf{A}}_t^- \\ &= i\mathcal{L}\mathcal{P}_t\tilde{\mathbf{A}}_t^-(\mathbf{q},\mathbf{p}) \ , \end{aligned} \tag{B3}$$

where we have again used the fact that $i\mathcal{L}$ commutes with $e^{\pm i\mathcal{L}t}$ and the projection at time t, $\mathcal{P}_t$. Equation (23) can now be derived by noting that for any observable $\mathbf{C}$:

$$i\mathcal{L}\mathcal{P}_t\mathbf{C}(\mathbf{q},\mathbf{p}) = i\mathcal{L}\mathbf{P}_t(\mathbf{q},\mathbf{p})\frac{\langle \mathbf{P}_t\mathbf{C}\rangle}{\langle \mathbf{P}_0^2\rangle} = \mathbf{F}_t(\mathbf{q},\mathbf{p})\frac{\langle \mathbf{P}_t\mathbf{C}\rangle}{\langle \mathbf{P}_0^2\rangle} \ . \tag{B4}$$

Applying this to $\mathbf{C}(\mathbf{q},\mathbf{p}) = \tilde{\mathbf{A}}_t^-(\mathbf{q},\mathbf{p})$, Eq. (B3) can be formally integrated from $\tilde{\mathbf{A}}_0^-(\mathbf{q},\mathbf{p}) = \mathbf{A}_0^-(\mathbf{q},\mathbf{p}) = \mathbf{A}_0(\mathbf{q},\mathbf{p})$ as

$$\tilde{\mathbf{A}}_t^-(\mathbf{q},\mathbf{p}) = \mathbf{A}_0(\mathbf{q},\mathbf{p}) + \int_0^t \mathbf{F}_u(\mathbf{q},\mathbf{p})\frac{\langle \mathbf{P}_u\tilde{\mathbf{A}}_u^-\rangle}{\langle \mathbf{P}_0^2\rangle}\,\mathrm{d}u \ . \tag{B5}$$

This can be rewritten, using $\mathbf{A}_t^- = e^{-i\mathcal{L}t}\tilde{\mathbf{A}}_t^-$ and the fact that $\langle \mathbf{P}_u\tilde{\mathbf{A}}_u^-\rangle = \langle \mathbf{P}_0\mathbf{A}_u^-\rangle$, as

$$\mathbf{A}_t^-(\mathbf{q},\mathbf{p}) = \mathbf{A}_0(\mathbf{q}^{-t},\mathbf{p}^{-t}) + \int_0^t \mathbf{F}_{u-t}(\mathbf{q},\mathbf{p})\frac{\langle \mathbf{P}_0\mathbf{A}_u^-\rangle}{\langle \mathbf{P}_0^2\rangle}\,\mathrm{d}u \tag{B6}$$

or, making the change of variable $u \to t-u$ in the integral,

$$\mathbf{A}_t^-(\mathbf{q},\mathbf{p}) = \mathbf{A}_{-t}(\mathbf{q},\mathbf{p}) + \int_0^t \mathbf{F}_{-u}(\mathbf{q},\mathbf{p})\frac{\langle \mathbf{P}_0\mathbf{A}_{t-u}^-\rangle}{\langle \mathbf{P}_0^2\rangle}\,\mathrm{d}u \ . \tag{B7}$$

[1] R. Zwanzig, *Nonequilibrium Statistical Mechanics* (Oxford University Press, Oxford, 2001).
[2] R. Zwanzig, Phys. Rev. **124**, 983 (1961).
[3] H. Mori, Prog. Theor. Phys. **33**, 423 (1965).
[4] J. Hynes, R. Kapral, and M. Weinberg, Physica A **80**, 105 (1975).
[5] H. Grabert, P. Hänggi, and P. Talkner, J. Stat. Phys. **22**, 537 (1980).
[6] T. Franosch, M. Grimm, M. Belushkin, F. M. Mor, G. Foffi, L. Forró, and S. Jeney, Nature (London) **478**, 85 (2011).

[7]X.-G. Wu and R. Kapral, J. Chem. Phys. **91**, 5528 (1989).
[8]D. Givon, R. Kupferman, and O. H. Hald, Isr. J. Math. **145**, 221 (2005).
[9]B. J. Berne and G. D. Harp, Adv. Chem. Phys. **17**, 63 (1970).
[10]G. R. Kneller and K. Hinsen, J. Chem. Phys. **115**, 11097 (2001).
[11]C. Hijón, P. Español, E. Vanden-Eijnden, and R. Delgado-Buscalioni, Faraday Discuss. **144**, 301 (2009).
[12]E. Darve, J. Solomon, and A. Kia, Proc. Natl. Acad. Sci. U.S.A. **106**, 10884 (2009).
[13]H. K. Shin, C. Kim, P. Talkner, and E. K. Lee, Chem. Phys. **375**, 316 (2010).
[14]D. Kauzlarić, P. Español, A. Greiner, and S. Succi, Macromol. Theor. Simul. **20**, 526 (2011).
[15]M. Berkowitz and W. Wan, J. Chem. Phys. **86**, 376 (1987).
[16]S. Koneshan, R. M. Lynden-Bell, and J. C. Rasaiah, J. Am. Chem. Soc. **120**, 12041 (1998).
[17]W. Smith and T. Forester, DLPOLY2 User Manual (Daresbury Laboratory, 2001).
[18]J. D. Weeks, D. Chandler, and H. C. Andersen, J. Chem. Phys. **54**, 5237 (1971).
[19]A. Carof, V. Marry, M. Salanne, J. Hansen, P. Turq, and B. Rotenberg, Mol. Simul. **40**, 237 (2014).
[20]J. T. Hynes, J. Chem. Phys. **59**, 3459 (1973).
[21]T. Yamaguchi, T. Matsuoka, and S. Koda, J. Chem. Phys. **122**, 014512 (2005).